Noble Metal Catalysts for Mercury Oxidation in Utility Flue Gas

GOLD, PALLADIUM AND PLATINUM FORMULATIONS

By Albert A. Presto and Evan J. Granite*

National Energy Technology Laboratory, United States Department of Energy, PO Box 10940, MS 58-106, Pittsburgh, PA 15236-0940, U.S.A.; *E-mail: evan.granite@netl.doe.gov

The use of noble metals as catalysts for mercury oxidation in flue gas remains an area of active study. To date, field studies have focused on gold and palladium catalysts installed at pilot scale. In this article, we introduce bench-scale experimental results for gold, palladium and platinum catalysts tested in realistic simulated flue gas. Our initial results reveal some intriguing characteristics of catalytic mercury oxidation and provide insight for future research into this potentially important process.

1. Introduction

Coal-fired utility boilers are the largest anthropogenic emitters of mercury in the United States, accounting for approximately one third of the 150 tons of mercury emitted annually (1, 2). In 2005, the U.S. Environmental Protection Agency (EPA) announced the Clean Air Mercury Rule, to limit mercury emissions from coal-fired utility boilers to 15 tons annually, approximately 30% of 1999 levels, by 2018 (3). At the time of publication (July 2008) this measure is under legal dispute. Of alternative legislative proposals to regulate mercury along with other pollutants, most would require a 90% mercury reduction, with deadlines for control varying from 2011 to 2015. Mercury exists in three forms in coal-derived flue gas: elemental (Hg^0), oxidised (Hg^{2+}) and particle-bound ($Hg_{(p)}$) (4). During combustion, mercury is liberated from coal as Hg^0. As the flue gas cools, some of the Hg^0 is oxidised, presumably to mercury(II) chloride ($HgCl_2$) because of the large excess of chlorine present in coal. Both Hg^0 and Hg^{2+} can enter the particulate phase by adsorption onto fly ash particles (5).

Hg^{2+} and $Hg_{(p)}$ are relatively easy to remove from flue gas using typical air pollution control devices. $Hg_{(p)}$ is captured, along with fly ash particles, in the particulate control device. Hg^{2+} is soluble in water, and is therefore removed with high efficiency by wet flue gas desulfurisation equipment (6). Hg^0, on the other hand, is difficult to capture. It is insoluble in water and is therefore not removed during flue gas desulfurisation. Activated carbon injection will remove both Hg^0 and Hg^{2+}, and currently this is the best method for removing Hg^0 from flue gas (6).

In addition to the Clean Air Mercury Rule, the U.S. EPA also enacted the Clean Air Interstate Rule, which requires reductions in NOx and SO_2 emissions in twenty-eight states (7). An expected consequence of this law is increased use of wet flue gas desulfurisation for SO_2 removal (8). Among the technologies being considered for mercury abatement in coal-fired boilers is therefore the combination of a catalyst and a wet scrubber; the catalyst oxidises Hg^0 to Hg^{2+}, and the oxidised mercury is subsequently absorbed by the scrubber solution. Catalysts capable of significant conversion (> 80%) of Hg^0 to Hg^{2+} could have tremendous value because the oxidised mercury can be removed concurrently with acid gases during flue gas desulfurisation.

Mercury oxidation catalysts can be employed in either of two configurations. In the 'co-benefit' application, selective catalytic reduction (SCR) catalysts with sufficient activity for mercury oxidation are installed upstream of a flue gas desulfurisation scrubber. The primary function of the SCR catalyst is to reduce NOx concentration in flue gas, and some power plants will need to install SCR to achieve compliance with the Clean Air Interstate
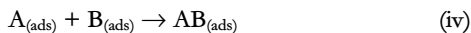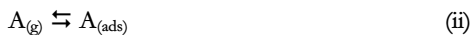
Rule (9). During operation, NO is reduced by NH$_3$, which is injected upstream of the SCR, at temperatures above 300°C. When the NH$_3$ is consumed (catalysts are typically oversized to prevent NH$_3$ slip), the catalyst is available for mercury oxidation.

Mercury oxidation catalysts can also be installed specifically for mercury control. In this case the catalyst is located downstream of the particulate control device, where the flue gas temperature is approximately 150°C. The lower temperature favours Hg^0 adsorption, and may therefore lead to more efficient mercury oxidation. Catalysts tested in this configuration include gold, palladium and vanadium-tungsten (10).

The catalytic oxidation of mercury to mercury(II) chloride typically assumes an overall reaction between Hg^0 and HCl, for example, Reaction (i):

$$Hg + 2HCl \rightarrow \rightarrow HgCl_2 \qquad (i)$$
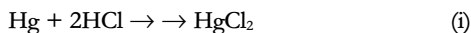
Cl$_2$ may also play a role in the formation of HgCl$_2$, but the equilibrium concentration of Cl$_2$ is only ~ 1% of the HCl concentration. Several key questions exist regarding this reaction. Specifically, the reaction mechanism is uncertain. The bimolecular reaction between two species adsorbed to a surface can be described by a Langmuir-Hinshelwood mechanism (11), Reactions (ii)–(v):
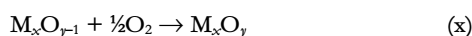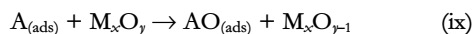
$$A_{(g)} \leftrightarrows A_{(ads)} \qquad (ii)$$

$$B_{(g)} \leftrightarrows B_{(ads)} \qquad (iii)$$

$$A_{(ads)} + B_{(ads)} \rightarrow AB_{(ads)} \qquad (iv)$$

$$AB_{(ads)} \rightarrow AB_{(g)} \qquad (v)$$

For this mechanism, the rate of reaction is dependent on the concentrations of reactants A and B, the adsorption equilibrium constant (K_i), and the rate constant for the surface reaction (k_{surf}). Mercury could also react *via* an Eley-Rideal mechanism, which is the reaction between a surface-bound species and a gas-phase (or weakly adsorbed) species, Reactions (vi)–(vii):

$$A_{(g)} \leftrightarrows A_{(ads)} \qquad (vi)$$

$$A_{(ads)} + B_{(g)} \rightarrow AB_{(g)} \qquad (vii)$$

Eley-Rideal and Langmuir-Hinshelwood mechanisms can be inferred by surface analysis of used

catalysts to confirm adsorption of specific reactants such as mercury and HCl. Additionally, pre-exposure of the catalyst to an oxidant, followed by mercury oxidation in the absence of the oxidant, would suggest either a Langmuir-Hinshelwood reaction or an Eley-Rideal reaction with the oxidant as the adsorbed species. A Langmuir-Hinshelwood mechanism can also be identified *via* chemical kinetics, though the relative adsorption behaviour of the reacting species may complicate analysis. In some cases, a Langmuir-Hinshelwood mechanism is characterised by a reaction that is first-order in each of the reactants (for example, Hg^0 and HCl). However, if one species saturates the surface, the reaction order with respect to the saturating species can be –1 (11).

Granite *et al.* (12) proposed that mercury oxidation could occur *via* a Mars-Maessen (13) mechanism. In this mechanism, adsorbed Hg^0 would react with a lattice oxidant (either O or Cl) that is replenished from the gas phase. Reactions (viii)–(xii) show the Mars-Maessen mechanism for the reaction of an adsorbed species (for example, Hg^0) with lattice oxygen:

$$A_{(g)} \leftrightarrows A_{(ads)} \qquad (viii)$$

$$A_{(ads)} + M_xO_y \rightarrow AO_{(ads)} + M_xO_{y-1} \qquad (ix)$$

$$M_xO_{y-1} + \tfrac{1}{2}O_2 \rightarrow M_xO_y \qquad (x)$$

$$AO_{(ads)} \rightarrow AO_{(g)} \qquad (xi)$$

$$AO_{(ads)} + M_xO_y \rightarrow AM_xO_{y+1} \qquad (xii)$$

The Mars-Maessen mechanism can be confirmed by the observation of mercury oxidation in the absence of gas-phase oxygen or chlorine, respectively (through variations of Reaction (ix)).

Medhekar *et al.* postulated that catalytically active mercury(II) chloride forms on the surfaces of many materials (14). They observed the reaction between elemental Hg and Cl$_2$ catalysed by Inconel® (an austenitic nickel-based alloy), quartz, stainless steel and Teflon®-coated stainless steel. Medhekar *et al.* found that many surfaces can catalyse the reaction between Hg and Cl$_2$ and that the surfaces are difficult to passivate with oxygen or fluorine. This suggests that the adsorbed HgCl$_2$ product is the actual catalyst. Ariya *et al.* observed

that the Hg + Cl₂ reaction proceeded faster when the reactor surface was covered with the reaction products of Hg + Br₂ than with a clean surface, suggesting a similar effect (15).

To date, none of the above mechanisms has been verified as the dominant mechanism for catalytic mercury oxidation. Mercury appears to react from an adsorbed state (10), but the phase of the HCl is uncertain. Furthermore, it is unknown whether Hg and HCl react directly, or if another species, such as mercury(II) oxide (HgO), is formed first (16, 17). The role of other flue gas species, specifically NO and SO_2, is unclear, and the behaviour of these species in mercury oxidation may depend strongly upon the nature of the catalyst. The deactivation mechanisms for the various mercury catalysts are also unknown.

In a previous article (10), we asserted that further research into the fundamental aspects of catalytic mercury oxidation is required to answer these significant questions. The information presented in this article is part of an ongoing effort toward that goal. We present initial results for mercury oxidation over three noble metal catalysts, Au, Pd and Pt. We envision that these materials could be used downstream of particulate control devices as mercury-specific catalysts. The results reveal several important aspects of the catalysts, and highlight some of the differences between Au and the platinum group metals (pgms) in mercury oxidation.

2. Experimental

Noble metal catalyst samples were exposed to mercury in a bench-scale packed bed reactor that has been described previously (18) and is shown schematically in Figure 1. The bench-scale assembly consisted of a quartz tube reactor, 22 mm internal diameter and 61 cm long, contained in a clamshell tube furnace. A catalyst bed containing approximately 0.5 g of catalyst was placed in the reactor and was supported by a quartz frit. Alumina beads were placed above the catalyst bed to ensure plug flow. A mass spectrometer was located downstream of the packed bed to monitor potential side reactions such as the formation of flue gas halides.
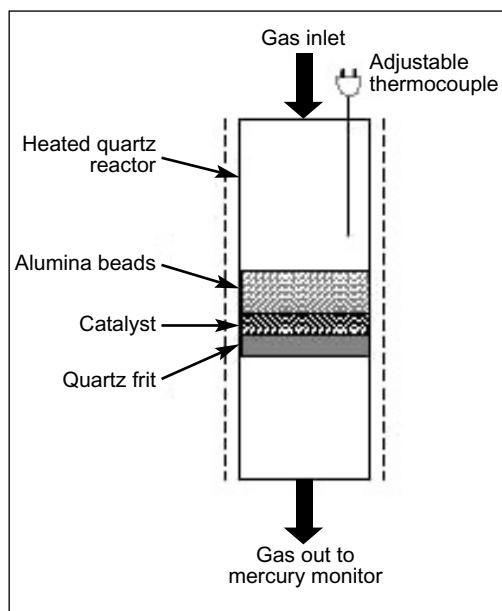

Fig. 1 Schematic diagram of the packed bed reactor

The catalysts used in this study were 1 wt.% Au, Pd and Pt, respectively, supported on 2 mm alumina beads (Johnson Matthey PLC). The BET surface area of the alumina beads was approximately 200 $m^2\ g^{-1}$. The catalysts were air calcined at elevated temperatures, thereby decomposing the precursor salts. It is very unlikely that the Au particles are of nanometre size because they sinter at the calcination temperatures. Therefore, the Au catalyst should have typical properties of bulk Au.

The mercury concentration and speciation exiting the packed bed were measured using a P S Analytical model 10.525 'Sir Galahad' continuous mercury monitor. A wet conditioning system with two channels for determining elemental and total mercury was placed upstream of the mercury monitor. The elemental mercury channel used an impinger filled with KCl solution to remove Hg^{2+} from the sample, and the total mercury channel used a $SnCl_2$/HCl solution to reduce Hg^{2+} to Hg^0. Both the KCl and $SnCl_2$/HCl impingers were followed by impingers containing $NaHCO_3$ solution that captured the acid gases SO_2 and HCl.

The mass of catalyst was selected to provide a small (10 to 50%) conversion of Hg^0 to Hg^{2+}. Very high or very low fractional conversions are unfavourable because they complicate the

interpretation of the experimental results. The precision of the mercury monitor used in this study is approximately 10 to 20% (1σ); therefore gas mixtures containing less than 10%, or more than 90%, oxidised mercury are statistically indisinguishable from gas mixtures that contain 0% or 100% oxidised mercury, respectively. The instrument precision is summed in quadrature for kinetics measurements, which require both elemental and oxidised mercury concentrations. The total uncertainty for the kinetics measurements is therefore 15 to 30% (Figure 2), and small fractional mercury conversions are nearly indistinguishable from the noise.

Difficulty in obtaining consistent mercury measurements in real or simulated flue gas at levels of parts per billion by volume is a common problem. For example, results from field studies indicate significant variability in mercury capture efficiency during activated carbon injection. Specifically, during long-term injection tests, individual measurements of mercury capture efficiency (timescale of minutes to hours) can differ significantly from the long-term results (timescale of months) (19). When all of the potential sources of experimental uncertainty are considered, it is our opinion that the precision presented here is appropriate for our experimental system, and is consistent with previous work from this laboratory (20).

The catalysts were exposed to simulated flue gas containing O_2, CO_2, HCl, SO_2, Hg^0 and N_2. Each catalyst sample was tested using the 'baseline' simulated flue gas detailed in Table I. The baseline

Table I			
Typical Simulated Flue Gas Conditions for the Experiments Conducted in This Study			
Parameter	Units	Baseline value	Range
$[O_2]$	%	5.25	0–5.25
$[SO_2]$	ppm	500	0–1000
$[NO]$	ppm	0	500
$[CO_2]$	%	12.5	–
$[HCl]$	ppm	50	0–100
$[CO]$	ppm	0	0–35
$[Hg]$	$\mu g\ Nm^{-3}$	10	6–18
Temperature	°C	149	138–160
Flow rate	slpm	8	8–10

conditions are roughly consistent with previous work from this laboratory, with the exception that NO was excluded from all but one experiment in this study because its presence interferes with mercury detection by the mercury monitor. The baseline conditions serve two purposes: first, they provide the basis for a like-for-like comparison for each of the catalysts tested. We will refer to the mercury oxidation rate measured in the presence of the baseline simulated flue gas as the 'baseline reaction rate'. The effects of excursions from the baseline gas composition are measured as deviations from the baseline reaction rate. Second, because the baseline conditions are used at the start of each experiment, they provide a way to measure catalyst deactivation over time.

Excursions from baseline conditions were undertaken in order to gain a more complete understanding of the reaction order with respect to
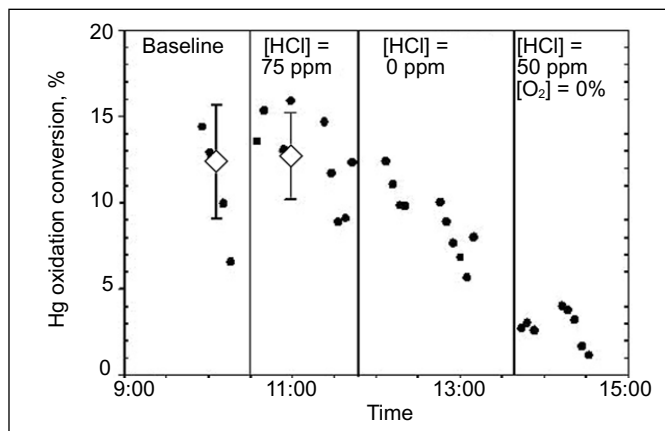

Fig. 2 Fractional mercury oxidation conversion across a gold catalyst as a function of time, from a typical experiment. The open symbols, ◇, indicate the average conversion for the baseline and [HCl] = 75 ppm time periods. Mercury conversion is expected to be nominally constant during these phases of the experiment. The error bars, I, show the 1σ level of precision

mercury and/or HCl, potential side or interfering reactions, and apparent activation energy. The effects of other flue gas species, such as SO_2 and CO, were also considered. These species can possibly bind to and deactivate the catalyst, or can participate in parallel reactions, such as flue gas halide formation, that may inhibit mercury oxidation.

The catalyst samples were tested for approximately six hours per day for several days. This procedure contrasts with packed bed experiments conducted by this group using mercury sorbents. In those experiments [18] the sorbent was exposed for six hours and removed from the packed bed reactor. The procedural difference between catalyst and sorbent experiments is intended to partially mimic the application of the two technologies in power plants: sorbents are typically injected and subsequently disposed of, whereas catalysts need to stay in place for months or years in order to be an economically viable option for mercury control [21]. Exposing the catalysts for multiple six-hour experiments also allows for an initial investigation into the flue gas species and/or processes that can deactivate the catalyst.

3. Results

The data presented in this article were analysed according to the chemical kinetics framework previously outlined by this group [22]. The catalysts are compared by considering the overall reaction rate for Hg^{2+} formation, measured in (mol Hg^{2+}) (g catalyst)$^{-1}$ s^{-1}. The results presented in this section focus specifically on the roles of HCl and oxygen in mercury oxidation.

A time series from a typical experiment is shown in Figure 3. In this experiment, the HCl and O_2 concentrations were changed in successive steps, and the mercury oxidation rate was measured following each change in simulated flue gas composition. Please note that the total concentration of mercury exiting the reactor bed, $[Hg^T]$, is equal to the concentration entering the reactor. This steady state, with no net adsorption of mercury, is typically referred to as 'complete breakthrough'. As with other studies of mercury oxidation catalysts, oxidation rate measurements were only made under conditions of complete breakthrough [22, 23].

At the start of the test series for each catalyst, the samples adsorbed mercury for two to six hours before reaching complete breakthrough. During most of the subsequent experiments, the catalyst sample adsorbed mercury for a short period, typically one hour, prior to reaching complete breakthrough. The mercury adsorbed during this start-up period likely replaced mercury that was desorbed during the cooldown period of the previous experiment.

During the first experiment for each catalyst, $Hg/CO_2/N_2$ and $Hg/CO_2/O_2/N_2$ gas mixtures were passed prior to the baseline simulated flue gas. All subsequent experiments were initiated with the baseline simulated flue gas (Table I). Complete mercury breakthrough occured quickly in the $Hg/CO_2/N_2$ atmosphere, and no mercury oxidation was evident in either of the mixtures. The onset of mercury oxidation coincided with the use of the baseline simulated flue gas.
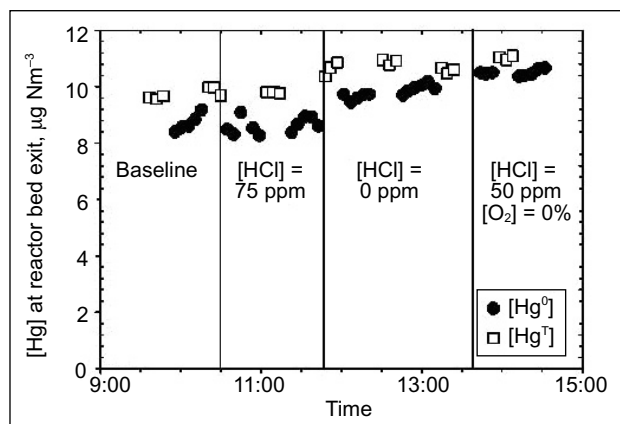

Fig. 3 Mercury monitor data showing mercury oxidation across a gold catalyst from a typical experiment. The simulated flue gas composition was changed from baseline conditions to high HCl (75 ppm), low HCl (0 ppm) and O_2-free conditions in successive steps. The system was allowed to reach an (apparent) steady state after each change to the simulated flue gas composition before another change was imposed. The oxidation rate was measured during the steady state portion of each time interval. $[Hg^T]$ = total mercury concentration

3.1 Gold Catalyst

The Au catalyst exhibited a consistent baseline rate of Hg^{2+} formation, as shown in Figure 4. The baseline reaction rate remained constant over a period of seven experiments, suggesting that there was no apparent catalyst deactivation. The mean baseline reaction rate was $(2.2 \pm 0.3) \times 10^{-10}$ (mol Hg^{2+}) (g catalyst)$^{-1}$ s^{-1}. The baseline reaction rate remained constant when the flow rate was raised from 8 standard litres per minute (slpm) to 10 slpm with no change in simulated flue gas composition. This result suggests that the mercury oxidation reaction is not limited by mass transfer under the conditions tested here.

The HCl concentration was varied from the baseline level of 50 parts per million (ppm) to 75 and 0 ppm. Raising the HCl concentration to 75 ppm had no effect on the reaction rate (Figure 2). Even though the reaction rate, and therefore the fractional conversion to oxidised mercury, were nominally constant during the baseline and elevated HCl portions of the experiment, the data in Figure 2 exhibit considerable scatter. As noted above, the precision for the kinetics measurements is approximately 15 to 30%. Due to the scatter in the data and the difficulty in making precise kinetic measurements with our current system, reaction rates reported here often represent time averages over periods of relative consistency (for example, the diamond symbols in Figure 2).

When the HCl concentration was set to 0 ppm, mercury oxidation continued, but the reaction rate slowed. The reaction rate fell to $\sim$ 85% of the baseline rate after 1.5 hours and $\sim$ 45% of the baseline rate after 2.5 hours. Time limitations prevented further testing, though we assume that mercury oxidation would have eventually stopped in the absence of an HCl source.

The mercury oxidation rate was also dependent on the presence of O_2. Removing O_2 from the simulated flue gas produced a similar effect to removing HCl: mercury oxidation continued at a reduced rate. Upon stopping O_2 flow, the Hg^{2+} formation rate fell to < 50% of the baseline rate. Mercury oxidation in the O_2-free simulated flue gas was only monitored for approximately 45 minutes, and as shown in Figure 2, the fractional mercury conversion was trending downward at the conclusion of the experiment. However, we are uncertain whether the reaction rate would have continued to decline as in the case of 0 ppm HCl.

In a separate experiment the temperature was varied from 138 to 160ºC. An apparent activation energy of 40 kJ mol^{-1} for the global reaction (i):

$$Hg + 2HCl \rightarrow \rightarrow HgCl_2 \qquad \text{(i)}$$
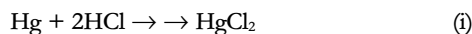
was calculated for this temperature range. This is consistent with the apparent activation energy of $\sim$ 30 kJ mol^{-1} measured by Zhao et al. (24) for the reaction of mercury with Cl_2 across a Au catalyst.

3.2 Palladium Catalyst

The baseline reaction rate across the Pd catalyst (Figure 4) declined over the course of the test period, falling from 1.6×10^{-10} to 3.3×10^{-11} (mol Hg^{2+}) (g catalyst)$^{-1}$ s^{-1}. Because of the rapid decline
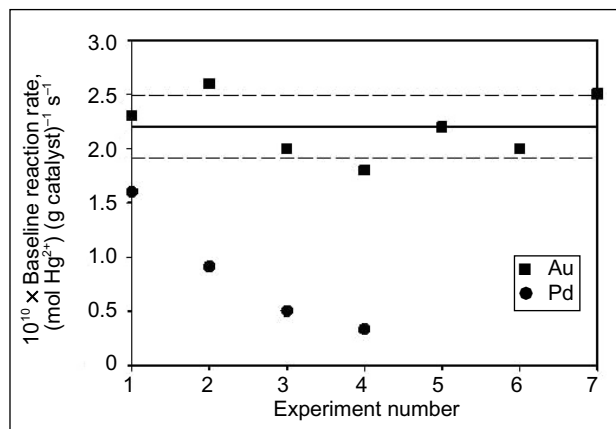

Fig. 4 *Baseline reaction rate across the gold (squares) and palladium (circles) catalysts for the experiments presented here. Experiments were conducted on consecutive days (excluding weekends), with one experiment per day. —— = the mean baseline reaction rate for the gold catalyst; — — — = one standard deviation*

in the baseline oxidation rate, all comparisons with the baseline rate are limited to a particular experiment. The baseline reaction rate was measured at the start of each experiment, and we assume that the baseline rate is roughly constant during a given experiment. The decrease in the baseline reaction rate with time suggests that the Pd catalyst is deactivated or fouled more readily than the Au catalyst.

The Pd catalyst exhibited similar responses to changes in HCl concentration to those of the Au catalyst. Raising the HCl concentration from 50 ppm to 100 ppm had no impact on the reaction rate. Lowering the HCl concentration to 0 ppm slowed, but did not halt, mercury oxidation. The oxidation rate fell to ~ 45% of the baseline rate after 80 minutes, and ~ 42% of the baseline rate after 150 minutes.

NO (500 ppm) was added for one experiment near the end of the test period. The baseline rate for this experiment was 3.3×10^{-11} (mol Hg^{2+}) (g catalyst)$^{-1}$ s^{-1}, and the mercury was approximately 10 to 20% oxidised downstream of the catalyst bed. Adding NO to the simulated flue gas reduced the sensitivity of the mercury monitor, and the observed total mercury concentration fell from 10 μg Nm^{-3} to 4 μg Nm^{-3}. With NO present, the mercury downstream of the catalyst bed was 90% oxidised. The reaction rate is not reported here because the measurement for the total Hg concentration is biased low. Regardless of the actual reaction rate, adding NO to the simulated flue gas resulted in significantly greater fractional mercury oxidation downstream of the catalyst bed.

3.3 Platinum Catalyst

As with the Pd catalyst, the baseline reaction rate observed with the Pt catalyst decreased over the course of the test period. The baseline rate fell from an initial maximum of 4.1×10^{-10} to 1.5×10^{-11} (mol Hg^{2+}) (g catalyst)$^{-1}$ s^{-1}. As with the Au and Pd catalysts, increasing the HCl concentration to 75 ppm and 100 ppm had no impact on the mercury oxidation rate. Reducing the HCl concentration to 0 ppm yielded an immediate halt to mercury oxidation. This behaviour is in contrast to that of the Au and Pd catalysts, both of which continued oxidising mercury at reduced rates when HCl flow stopped.

Prior to one experiment the Pt catalyst was reduced at 165ºC with 60 ppm CO in N_2. The catalyst was then exposed to a mixture of Hg/CO_2/HCl/SO_2/N_2 at 150ºC. No oxidised mercury formation was observed. When O_2 was added to the gas mixture to form the baseline simulated flue gas, mercury oxidation was evident. The HCl flow was then stopped, with the expectation that mercury oxidation would again stop. Instead, oxidation continued at a reduced rate, consistent with the behaviour observed for the Au and Pd catalysts.

The apparent activation energy for mercury oxidation across the Pt catalyst was measured for the temperature range 140 to 157ºC. The measured activation energy was ~ 120 kJ mol^{-1}, significantly higher than that measured for the Au catalyst.

4. Discussion

As stated in the Introduction, previous investigations of mercury oxidation over a variety of catalysts indicate that mercury reacts from a bound state, for example, $Hg_{(ads)}$. It is well established that mercury adsorbs to Au, Pt and Pd surfaces. Gold (25, 26), palladium (27) and iridium (28) have all been used as modifiers for improving mercury capture in graphite tube atomic absorption spectrometry. The mercury monitor used in this study removes mercury vapour from the sample gas using Au/sand traps. The captured mercury is thermally desorbed during the analysis step of the instrument cycle. Mercury is also known to adsorb to Pt and form a solid solution with it (29). Therefore, we are confident in assuming that mercury adsorbs to the catalyst surface prior to reacting.

The dependence of the mercury oxidation rate on the presence of HCl in the simulated flue gas suggests that the oxidised mercury species observed by the mercury monitor is indeed $HgCl_2$. Mercury oxidation was not observed when the catalyst was exposed to the Hg/CO_2/O_2/N_2 gas mixture used prior to the simulated flue gas, indicating that the observed oxidised mercury species is unlikely to be HgO. Mercury(I) chloride (Hg_2Cl_2) is also a possibility, as it can form *via* the Boliden-Norzink reaction (30), Reaction (xiii):

$$Hg(g) + HgCl_2 \rightarrow Hg_2Cl_2 \qquad (xiii)$$

However, thermodynamic calculations indicate that Hg_2Cl_2 is not stable under typical flue gas conditions (31).

For all three noble metal catalysts tested here, increasing the HCl concentration above 50 ppm had no impact on the reaction rate. In a previous study, we made an initial assumption that the mercury oxidation rate can be described by $r = k[Hg][HCl]$ (22). This assumption is obviously false for HCl concentrations > 50 ppm.

The assumption above required Hg + HCl as participants in the rate-limiting step. At this point, the rate-limiting step is unclear. When HCl was removed from the simulated flue gas during the tests with the Au and Pd catalysts, the reaction rate immediately fell, suggesting that the lack of a chlorine source to replenish the surface reduced the reaction rate. Mulla *et al.* suggested that the adsorption of O_2 to an empty surface site was the rate-limiting step for NO oxidation over a Pt/Al_2O_3 catalyst (32). Perhaps this step is also rate-limiting for the formation of the presumed HgO intermediate product detailed below.

The data for the Au and Pd catalysts suggest that mercury reacts with HCl that is bound to the catalyst surface. This explains why mercury oxidation continues in the absence of gas-phase HCl, but with a declining reaction rate. Cl_2 can chemisorb to Au surfaces and form $AuCl_3$ (33). HCl dissociatively adsorbs to Pt surfaces (34), and similar behaviour might be expected for Pd. Thus, surface-bound Cl should be available for reaction on the Au and Pd surfaces.

The Pt catalyst exhibited different behaviour in the absence of HCl, and mercury oxidation stopped. This might be evidence of an Eley-Rideal mechanism for mercury oxidation across the Pt catalyst, with adsorbed Hg (or an intermediate such as HgO, described below) reacting with gas-phase HCl. Eley-Rideal kinetics would not suggest the zero-order dependence on [HCl] for concentrations greater than 50 ppm, but the overall reaction could exhibit a zero-order dependence on [HCl] if the $Hg_{(ads)} + HCl_{(g)}$ step is not rate-limiting.

In a chlorine- and sulfur-free flame, Schofield (16, 17) observed HgO deposition on Pt and stain- less steel surfaces. When HCl was added to the flame, the HgO desorbed as $HgCl_2$. The implication of this observation is that Hg and HCl do not react directly to form $HgCl_2$, but rather form *via* a HgO intermediate. Pt is an effective adsorber of oxygen (32, 35–37), hence surface-bound oxygen should be present in excess for the conversion of $Hg^0_{(g)}$ to $HgO_{(ads)}$. In the absence of $HCl_{(g)}$, the HgO remains bound to the surface because of its low vapour pressure. When HCl is present, the HgO is converted to $HgCl_2$, which desorbs from the surface and allows more Hg to react. The vapour pressure of $HgCl_2$ is sufficiently high (1 Torr at 136ºC), and the concentration is sufficiently low, that the simulated flue gas stream can hold $HgCl_2$ as a vapour even at temperatures well below the sublimation point.

We tested the Schofield hypothesis in the experiment that used the reduced Pt catalyst. This test yielded two important results: (a) O_2 and HCl (or possibly Cl_2) are required for mercury oxidation across a Pt catalyst, possibly because $HgCl_2$ formation is preceded by HgO; (b) the Pt catalyst can display a significant history effect.

In the initial series of experiments, the catalyst was exposed to an O_2-containing gas mixture prior to the introduction of HCl. In the experiment with the reduced Pt, the catalyst was exposed to HCl prior to O_2. We hypothesise that in the initial tests, $O_{(ads)}$ greatly outnumbers $Cl_{(ads)}$ to the point of exclusion. Thus, HgO is easily formed on the surface, and HCl reacts with the adsorbed HgO from the gas phase. Without HCl, there is no chlorine source for $HgCl_2$ formation. In the experiment using the reduced Pt, the initial exposure to HCl allows for an ample concentration of adsorbed chlorine that is joined by adsorbed oxygen when O_2 is introduced. When HCl is removed from the simulated flue gas, there is sufficient surface-bound chlorine to sustain $HgCl_2$ formation at a reduced rate. The reaction mechanism remains unclear. The initial experiments suggest the possibility of an Eley-Rideal mechanism, and the experiments with the reduced Pt catalyst might suggest a Langmuir-Hinshelwood mechanism.

The data suggest that mercury oxidation across the Au catalyst is dependent on the presence of O_2.

This behaviour, while puzzling, may indicate the formation of the HgO intermediate. HgO binds to Au surfaces, and density functional theory calculations indicate that the binding energy for mercury species on Au(001) decreases in the series: HgO > Hg^0 > $HgCl_2$ (38). The predicted energy of binding of $HgCl_2$ to the Au(001) surface is only 17.2 kJ mol^{-1}, suggesting that this species could easily desorb from the catalyst surface at the temperatures tested here.

The mechanism governing the oxygen dependence of mercury oxidation across the Au catalyst is unknown at this time. Unlike with Pt, oxygen is not expected to efficiently adsorb to the Au surface (39), suggesting that adsorbed oxygen for HgO formation is not readily available at the surface. One could postulate an Eley-Rideal reaction between bound Hg and $O_{2(g)}$ to form HgO, but this reaction requires accounting for the second oxygen atom, suggesting either a ternary reaction (xiv):

$$2Hg + O_2 \rightarrow 2HgO \qquad \text{(xiv)}$$

which is unlikely, or the migration of an oxygen atom to the Au surface, which is also unlikely. Further research is required to elucidate this behaviour.

The nature of the bonding of mercury, chlorine and oxygen species to the catalyst surface is unknown at this time. One possibility is that each species adsorbs to the surface individually – $Hg_{(ads)}$, $Cl_{(ads)}$, $HgO_{(ads)}$, etc. Mercury is known to interact with other metals to form a variety of oxides and halides (40) that could participate in the surface reactions which lead to the formation of $HgCl_2$. Surface analysis of fresh and used catalyst samples will be conducted in the future in order to gain more insight.

The most significant difference between the performance of the Au and the pgm catalysts, was the loss of catalytic activity for the Pd and Pt over the course of the test period. The presence of adsorbed oxygen on the catalyst surface may offer an explanation for the observed drop in catalyst activity. While testing Pt/Al_2O_3 catalysts for the oxidation of NO to NO_2, Mulla et al. observed that the catalyst deactivated during cooldown and other changes to process conditions (32). The

researchers proposed that deactivation may have been the result of the oxidation of the Pt surface. Olsson et al. also observed deactivation of Pt/Al_2O_3 and $Pt/BaO/Al_2O_3$ catalysts during the same reaction and attributed the loss of catalytic activity to the formation of unreactive PtO (41). The formation of Pt and Pd oxides, especially while exposed to O_2 during cooldown, may also explain the deactivation observed here. The poor reactivity of PtO might also suggest that the possible HgO intermediate product is not formed via a Mars-Maessen reaction. Au, on the other hand, is typically a poor adsorber of oxygen and is likely not subject to this deactivation mechanism (39).

Mulla et al. found that their Pt/Al_2O_3 catalyst could be regenerated with CO or H_2 (32). This observation agrees well with the data presented here; Hg oxidation proceeded at nearly the initially observed baseline reaction rate after the Pt catalyst was exposed to CO. The enhanced extent of Hg oxidation observed across the Pd catalyst in the presence of NO also suggests that surface oxygen inhibits Hg oxidation. When NO was added to the simulated flue gas used here, it is possible that surface oxygen was removed, allowing for increased conversion of mercury (32, 35–37, 41).

It is unclear at this time whether the Pt and Pd catalysts were deactivated by the formation of oxides (for example, PtO and PdO), surface-bound oxygen, or both. While NO may have removed adsorbed oxygen from the Pd surface, the presence of PtO has been observed to inhibit NO oxidation across Pt catalysts (41). Thermal regeneration of Pt catalysts requires temperatures of 600 to 650°C, significantly higher than the temperatures used here. Surface analysis will be required to confirm the nature of the catalyst surface following exposure to the simulated flue gas.

Of concern with all potential mercury oxidation catalysts are the unwanted side reactions (xv) and (xvi):

$$NO + \tfrac{1}{2}O_2 \rightarrow NO_2 \qquad \text{(xv)}$$

and

$$SO_2 + \tfrac{1}{2}O_2 \rightarrow SO_3 \qquad \text{(xvi)}$$

Stack NO_2 concentrations as low as 15 ppm (42) can lead to the formation of a brown plume and enhanced local ozone production. SO_3 is captured poorly in most wet flue gas desulfurisation systems, and can lead to sulfuric acid mist in the downstream plume. In each case, a small concentration can produce a significant impact – 15 ppm NO_2 corresponds to only 3% NO conversion for flue gas containing 500 ppm NO. To date, both Au and Pd catalysts have been tested at pilot scale, and neither SO_3 nor NO_2 formation was observed (23). However, formation of these unwanted by-products remains a concern.

The results introduced here may have several implications for the use of noble metal catalysts in mercury abatement schemes. Perhaps most important is the observation that Au exhibits superior resistance to deactivation than Pd and Pt. Contrary to our short-term, bench-scale results, pilot-scale testing of Au and Pd showed similar performance and deactivation over time (23). A likely explanation is the presence of NO in the real flue gas; as shown here, NO appears to regulate the surface oxygen concentration on the Pd catalyst, leading to improved Hg oxidation *versus* a NO-free simulated flue gas. The oxygen resistance of Au may come into play during periods of down time, when the catalyst beds come into contact with air at ambient temperature. This condition favours oxygen adsorption onto Pt and Pd. However, a preference for Au remains to be seen, and future, longer-term testing may be warranted.

5. Conclusions

The results presented here provide an initial investigation into the mechanisms behind mercury oxidation across noble metal catalysts, and more work is needed. Investigations are needed into the role of other potential flue gas catalyst poisons such as arsenic, selenium and SO_3. Selenium is suspected to deactivate Au catalysts tested at pilot scale (23), and initial experiments conducted in our laboratory suggest that high concentrations of SO_3 can deactivate Au catalysts. Future work should also focus on the possible beneficial role of different promoters, alloys and supports. At the size and timescale presented here, both Au and pgms show

promise for use as mercury oxidation catalysts. As we begin to understand mercury oxidation across these catalysts – specifically the roles of O_2 and HCl and the apparent deactivation mechanisms – improvements can be made that will help mercury oxidation catalysts become economically competitive as part of a mercury abatement strategy.

Disclaimer

References in this paper to any specific commercial product, process, or service are to facilitate understanding, and do not necessarily imply its endorsement by the U.S. DOE.

References

1 "Mercury Study Report to Congress", U.S. EPA, U.S. Government Printing Office, Washington, D.C., December, 1997:
   http://www.epa.gov/mercury/report.htm

2 "Study of Hazardous Air Pollutant Emissions from Electric Utility Steam Generating Units – Final Report to Congress", U.S. EPA, U.S. Government Printing Office, Washington, D.C., February, 1998: http://www.epa.gov/ttn/oarpg/t3/reports/eurtc1.pdf

3 'Clean Air Mercury Rule', U.S. EPA, 15th March, 2005: http://www.epa.gov/camr/

4 K. C. Galbreath and C. J. Zygarlicke, *Environ. Sci. Technol.*, 1996, **30**, (8), 2421

5 C. L. Senior and S. A. Johnson, *Energy Fuels*, 2005, **19**, (3), 859

6 J. H. Pavlish, E. A. Sondreal, M. D. Mann, E. S. Olson,

K. C. Galbreath, D. L. Laudal and S. A. Benson, *Fuel Proc. Technol.*, 2003, **82**, (2–3), 89

7 'Clean Air Interstate Rule', U.S. EPA, 10th March, 2005: http://www.epa.gov/cair/

8 R. K. Srivastava, N. Hutson, B. Martin, F. Princiotta and J. Staudt, *Environ. Sci. Technol.*, 2006, **40**, (5), 1385

9 R. K. Srivastava, R. E. Hall, S. Khan, K. Culligan and B. W. Lani, *J. Air Waste Manage. Assoc.*, September, 2005, **55**, (9), 1367

10 A. A. Presto and E. J. Granite, *Environ. Sci. Technol.*, 2006, **40**, (18), 5601

11 M. J. Pilling and P. W. Seakins, "Reaction Kinetics", 2nd Edn., Oxford University Press, Oxford, U.K., 1995

12 E. J. Granite, H. W. Pennline and R. A. Hargis, *Ind. Eng. Chem. Res.*, 2000, **39**, (4), 1020

13 P. Mars and J. G. H. Maessen, *J. Catal.*, 1968, **10**, (1), 1

14 A. K. Medhekar, M. Rokni, D. W. Trainor and J. H. Jacob, *Chem. Phys. Lett.*, 1979, **65**, (3), 600

15 P. A. Ariya, A. Khalizov and A. Gidas, *J. Phys. Chem. A*, 2002, **106**, (32), 7310

16 K. Schofield, *Chem. Phys. Lett.*, 2004, **386**, (1–3), 65

17 K. Schofield, *Proc. Combust. Inst.*, 2005, **30**, (1), 1263

18 A. A. Presto and E. J. Granite, *Environ. Sci. Technol.*, 2007, **41**, (18), 6579

19 S. Nelson, "Brominated Sorbents for Small Cold-Side ESPs, Hot-Side ESPs, and Fly Ash Use in Concrete", Progress Report to U.S. DOE/NETL, Cooperative Agreement No. DE-FC26-05NT42308, Sorbent Technologies Corporation, 2007

20 E. J. Granite and H. W. Pennline, *Ind. Eng. Chem. Res.*, 2002, **41**, (22), 5470

21 G. Blythe, "Pilot Testing of Mercury Oxidation Catalysts for Upstream of Wet FGD Systems", Quarterly Technical Progress Report to U.S. DOE/NETL, U.S. Department of Energy Agreement No. DE-FC26-01NT41185, URS Corporation, 2003

22 A. A. Presto, E. J. Granite, A. Karash, R. A. Hargis, W. J. O'Dowd and H. W. Pennline, *Energy Fuels*, 2006, **20**, (5), 1941

23 G. Blythe, K. Dombrowski, T. Machalek, C. Richardson and M. Richardson, "Pilot Testing of Mercury Oxidation Catalysts for Upstream of Wet FGD Systems", Final Report to U.S. DOE/NETL, U.S. Department of Energy Agreement No. DE-FC26-01NT41185, URS Corporation, 2006

24 Y. Zhao, M. D. Mann, J. H. Pavlish, B. A. F. Mibeck, G. E. Dunham and E. S. Olson, *Environ. Sci. Technol.*, 2006, **40**, (5), 1603

25 Z. Hladky, J. Rísová and M. Fisera, *J. Anal. At. Spectrom.*, 1990, **5**, (8), 691

26 J. P. Matousek, R. Iavetz, K. J. Powell and H. Louie, *Spectrochim. Acta Part B.: At. Spectrom.*, 2002, **57**, (1), 147

27 X.-P. Yan and Z.-M. Ni, *Anal. Chim. Acta*, 1993, **272**, (1), 105

28 B. Radziuk and J. Kleiner, *Spectrochim. Acta Part B: At. Spectrom.*, 1993, **48**, (14), 1719

29 F. L. Fertonani, A. V. Benedetti and M. Ionashiro, *Thermochim. Acta*, 1995, **265**, 151

30 T. Allgulin, Boliden AB, *U.S. Patent* 3,849,537; 1974

31 F. Frandsen, K. Dam-Johansen and P. Rasmussen, *Prog. Energy Combust. Sci.*, 1994, **20**, (2), 115

32 S. S. Mulla, N. Chen, L. Cumaranatunge, G. E. Blau, D. Y. Zemlyanov, W. N. Delgass, W. S. Epling and F. H. Ribeiro, *J. Catal.*, 2006, **241**, (2), 389

33 N. D. Spencer and R. M. Lambert, *Surf. Sci.*, 1981, **107**, (1), 237

34 F. T. Wagner and T. E. Moylan, *Surf. Sci.*, 1989, **216**, (3), 361

35 J. Després, M. Elsener, M. Koebel, O. Kröcher, B. Schnyder and A. Wokaun, *Appl. Catal. B: Environ.*, 2004, **50**, (2), 73

36 R. Marques, P. Darcy, P. Da Costa, H. Mellottée, J.-M. Trichard and G. Djéga-Mariadassou, *J. Mol. Catal. A: Chem.*, 2004, **221**, (1–2), 127

37 M. F. Irfan, J. H. Goo, S. D. Kim and S. C. Hong, *Chemosphere*, 2007, **66**, (1), 54

38 E. Sasmaz and J. Wilcox, 'The Binding of Flue Gas Components on CaO, TiO$_2$, Pd, Au and PdAu Alloy', Paper No. 409, in "Proceedings of the Air & Waste Management Association's 100th Annual Conference and Exhibition", Pittsburgh, PA, June, 2007, A&WMA, Pittsburgh, PA, 2007

39 X. Deng, B. K. Min, A. Guloy and C. M. Friend, *J. Am. Chem. Soc.*, 2005, **127**, (25), 9267

40 J. W. Mellor, "A Comprehensive Treatise on Inorganic and Theoretical Chemistry", Longmans, Green and Company, London, New York, 1952, Vol. IV

41 L. Olsson and E. Fridell, *J. Catal.*, 2002, **210**, (2), 340

42 A. S. Feitelberg and S. M. Correa, *J. Eng. Gas Turbines Power*, 2000, **122**, (2), 287

The Authors

Dr Albert A. Presto is currently a Research Scientist and Laboratory Manager for the Air Quality Laboratory in the Center for Atmospheric Particle Studies at Carnegie Mellon University. Prior to his current position he was an ORISE postdoctoral fellow at the U.S. Department of Energy's National Energy Technology Laboratory (NETL) in Pittsburgh. His research interests include mercury removal from coal-derived flue and fuel gas, atmospheric secondary organic aerosol formation, the atmospheric processing of organic aerosol, and atmospheric radical chemistry.

Dr Evan J. Granite is a Research Group Leader at the NETL. His research has focused on mercury and carbon dioxide removal from flue and fuel gases. Dr Granite is the principal investigator for three projects on the capture of mercury, arsenic and selenium from coal-derived flue and fuel gases, and carbon dioxide separation from flue gas. His research interests are in catalysis and surface chemistry, pollution clean-up, electrochemistry and photochemistry.